

# Probing the quantum state of a guided atom laser pulse

Kevin L. Moore,\* Subhadeep Gupta, Kater W. Murch, and Dan M. Stamper-Kurn

*Department of Physics, University of California, Berkeley CA 94720*

(Dated: May 26, 2018)

We describe bichromatic superradiant pump-probe spectroscopy as a tomographic probe of the Wigner function of a dispersing particle beam. We employed this technique to characterize the quantum state of an ultracold atomic beam, derived from a  $^{87}\text{Rb}$  Bose-Einstein condensate, as it propagated in a 2.5 mm diameter circular waveguide. Our measurements place an upper bound on the longitudinal phase-space area occupied by the  $3 \times 10^5$  atom beam of  $9(1)\hbar$  and a lower bound on the coherence length ( $\mathcal{L} \geq 13(1) \mu\text{m}$ ). These results are consistent with full quantum degeneracy after multiple orbits around the waveguide.

Advances in the control of quantum degenerate gases have mirrored those of optical lasers, including the realization of high-contrast atom interferometers [1, 2], nonlinear atom optics [3] and dispersion management [4, 5]. Further, given single-mode waveguides for atoms [6] and other atom optical elements, the prospect of sensitive guided-atom interferometry has invited intensive experimental pursuit. Critical to realizing this prospect are methods for characterizing the coherence of a guided atom beam, analogous to beam characterization in a high-energy particle accelerator.

Pulsed particle beams are naturally described by the Wigner quasi-probability distribution, defined as [7]

$$\mathcal{W}(\mathbf{r}, \mathbf{p}) = \frac{1}{2\pi} \int e^{-i\mathbf{p}\cdot\mathbf{y}/\hbar} \langle \mathbf{r} - \frac{\mathbf{y}}{2} | \hat{\rho} | \mathbf{r} + \frac{\mathbf{y}}{2} \rangle d\mathbf{y}, \quad (1)$$

with  $\hat{\rho}$  being the density matrix of the system. This distribution is the quantum mechanical equivalent of the classical phase-space distribution. Experimentally,  $\mathcal{W}(\mathbf{r}, \mathbf{p})$  is determined tomographically by measuring its projection at various angles in phase space [8, 9].

In this Letter we describe the use of bichromatic superradiant pump-probe spectroscopy (SPPS) to quantify the coherence of a dispersing atomic beam propagating in a circular waveguide [10]. We show how the waveguide curvature allows for tomographic measurements of the Wigner function of the beam and, thereby, for an accurate measurement of its phase-space density. Both long-range coherence and single transverse mode propagation were evident over many revolutions of atoms in the waveguide, implying that a guided atom laser pulse derived from a Bose-Einstein condensate remains coherent for at least 300 ms of propagation.

Superradiant light scattering from quantum degenerate gases provides striking confirmation of their long-range coherent nature [11, 12]. An elongated cloud undergoing superradiance scatters light preferentially into “end-fire modes,” leading to highly directional emission [13]. Coherence between scattered and unscattered atoms establishes

a periodic grating of density or polarization which stimulates further light scattering. Once established, whether by superradiance or otherwise [14, 15], this grating will decay or dephase on a timescale  $\tau_c = m/2|\mathbf{q}|\sigma_p$  with  $m$  being the atomic mass,  $\hbar\mathbf{q}$  the superradiant scattering recoil momentum and  $\sigma_p$  the rms momentum spread of the unscattered atoms along the recoil direction. The decay of coherence can be isolated experimentally by applying superradiance in a pump-probe manner. After a first optical pump pulse initiates superradiance and establishes coherence in the gas, this coherence is allowed to decay freely for a time  $\tau$  before a second optical pulse is applied. In Ref. [12], this pump-probe technique revealed in detail the bimodal momentum distribution of a partly-condensed Bose gas.

Let us consider an elongated beam of  $N$  atoms in the transverse ground state of a 1D waveguide with longitudinal rms spatial and momentum widths of  $\sigma_x$  and  $\sigma_p$ , respectively. The 1D Wigner function of the beam is bounded by these widths to occupy a phase-space area no larger than  $\mathcal{A}_{max} = \sigma_x \sigma_p$ . However,  $\mathcal{A}_{max}$  may represent a gross overestimate of the actual phase space area occupied by the beam. For example, consider that the beam originates from a thermally-equilibrated trapped gas that was released into the waveguide. Free expansion of the gas causes the momentum and position of the beam to be strongly correlated, a feature captured by a posited Wigner function of the form

$$\mathcal{W}(x, p) = \frac{\exp\left[-\frac{1}{2(1-\eta^2)}\left(\frac{x^2}{\sigma_x^2} - 2\eta\frac{xp}{\sigma_x\sigma_p} + \frac{p^2}{\sigma_p^2}\right)\right]}{\pi\sigma_x\sigma_p\sqrt{1-\eta^2}} \quad (2)$$

where  $\eta = \langle px \rangle / \sigma_p \sigma_x$  (Fig. 1). The actual phase-space area  $\mathcal{A}$  occupied by such a beam is smaller than the aforementioned estimate by a factor  $\sqrt{1-\eta^2}$ . That is, for proper characterization of an atomic beam one must distinguish between a spatially-inhomogeneous momentum width  $\sigma_p$ , which may be dominated by a coherent velocity chirp across the length of the beam, and a “homogeneous” width  $\mathcal{A}/\sigma_x$ .

To access these correlations, we consider *bichromatic* SPPS in which the recoil momenta  $\hbar\mathbf{q}_1$  and  $\hbar\mathbf{q}_2$  imparted by superradiance are different for the pump and probe

\*Electronic address: klmoores@berkeley.edu

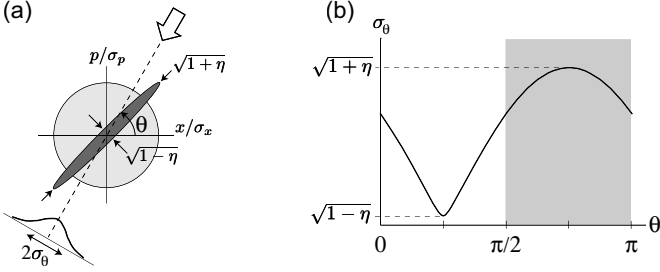


FIG. 1: Projective measurements as probes of quantum degeneracy. (a) Contours of Gaussian Wigner distributions  $\mathcal{W}(x, p)$  are shown.  $\mathcal{W}(x, p)$  is determined by its projections at all angles  $0 \leq \theta < \pi$ . Measurements of only the momentum and position distributions ( $\theta = 0$  and  $\theta = \pi/2$  projections, respectively), cannot distinguish a homogeneous (light shading) from a correlated ensemble (dark shading). (b) rms widths of distributions derived at various projection angles are shown. Time-of-flight analyses recover a limited range of projection angles (shaded), while bichromatic SPPS accesses all projection angles.

pulses, respectively (Fig. 2a-b). These differing momenta may result experimentally from pump and probe pulses which differ in wavevector, or, as in the present experiment, which differ in their angle of incidence with respect to the long axis of the cloud. Restricting our treatment to one dimension along  $\hat{x}$ , the superradiant scattering rate  $\Gamma$  from the second (probe) light pulse [11, 16] can be expressed in terms of the Wigner function of the state of the system *before* the first (pump) pulse as

$$\Gamma \propto \left| \iint e^{i\left(\frac{q_1 \tau}{m} p + \Delta q x\right)} \mathcal{W}(x, p) dx dp \right|^2. \quad (3)$$

where  $\Delta q = q_2 - q_1$  with  $\hbar q_1$  and  $\hbar q_2$  being the projections of the recoil momenta along the  $\hat{x}$  axis, and  $\tau$  is the pump-probe delay time. Performing an extended canonical transformation to generalized coordinates  $\tilde{x} = (x/\sigma_x) \cos \theta + (p/\sigma_p) \sin \theta$  and  $\tilde{p} = -(x/\sigma_x) \sin \theta + (p/\sigma_p) \cos \theta$ , with  $\tan \theta = -\frac{\Delta q m}{q_1 \tau} \frac{\sigma_x}{\sigma_p}$  we obtain

$$\Gamma \propto \left| \int e^{i\left(\frac{\sigma_p q_1 \tau}{m} \cos \theta - \sigma_x \Delta q \sin \theta\right) \tilde{p}} d\tilde{p} \int \mathcal{W}(x, p) d\tilde{x} \right|^2. \quad (4)$$

Monochromatic SPPS ( $\Delta q = 0$ ) yields information only on the overall momentum distribution of the atomic system, which derives from projecting the Wigner function on the momentum axis ( $\theta = 0$ ) [12]. In contrast, bichromatic SPPS assesses the Wigner function at a non-zero projection angle  $\theta$ . In particular, tuning experimental parameters such that  $\theta = \pi/4$  probes the Wigner function of Eq. 2 along the narrow axis corresponding to the linear momentum chirp across the cloud, and thereby provides a sensitive measurement of  $\eta$  and of the phase-space density of the beam.

In other words, in monochromatic SPPS the reduction of the superradiant scattering rate from a linearly-chirped

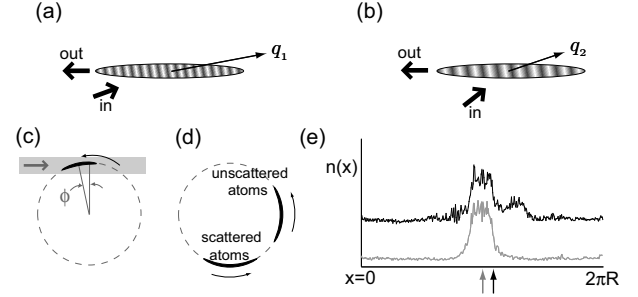


FIG. 2: Bichromatic SPPS in a circular waveguide. (a) Superradiant Rayleigh scattering of a pump pulse establishes a density modulation of wavevector  $\hbar \mathbf{q}_1$  in an elongated atomic beam. (b) A coherent velocity chirp causes the modulation wavevector to decrease along the long axis. The remaining coherence is revealed by light scattering with recoil momentum  $\hbar \mathbf{q}_2$  matched to the modified density grating. (c) Pump (probe) light illuminates the freely propagating atom beam at angle  $\phi$  ( $\phi + \Omega \tau$ ) relative to the mean angular position, and (d) scattered atoms separate from the original pulse and can be distinguished from unscattered atoms. (e) Azimuthal density distributions  $n(x)$  in the ring 160 ms after illumination are shown for beams that have (black) or have not (grey) undergone superradiant light scattering. The shifted center of mass (indicated by arrows) quantifies the total superradiant scattering rate.

beam comes about mainly by dephasing. The density modulation established by the pump pulse evolves at a frequency which is Doppler-shifted upward on one end and downward on the other end of the momentum-chirped beam. Over time, this causes the wavevector of the density modulation to decrease linearly with time. In bichromatic SPPS, by matching the recoil momentum of the probe pulse to the wavevector of the density grating, we recover a superradiant scattering rate which reveals the remaining homogeneous decay of motional coherence.

We now turn to our implementation of this scheme to probe a pulsed atom laser beam in a circular waveguide. This beam originated from a  $^{87}\text{Rb}$  Bose-Einstein condensate of  $3 \times 10^5$  atoms produced in a magnetic time-orbiting ring trap (TORT) [10, 17], biased to yield a three-dimensional harmonic trap with trapping frequencies  $(\omega_x, \omega_T) = 2\pi \times (35, 85) \text{ s}^{-1}$  in the axial (i.e. azimuthal in the ring) and transverse directions, respectively. These atoms were launched azimuthally by adiabatically decompressing the trap to  $\omega_x = 2\pi \times 6 \text{ s}^{-1}$  and displacing the trap minimum to a new longitudinal position for 30 ms, accelerating the cloud to a mean orbital angular frequency  $\Omega = 2\pi \times 8.4 \text{ s}^{-1}$  chosen to be far from any betatron resonances [17]. The TORT potential was then balanced over the next 30 ms and operated with radius  $R = 1.25 \text{ mm}$  and  $\omega_T$  as above. The launched atomic beam was allowed to propagate freely in this circular guide.

While in the particular case examined, the beam's provenance as a Bose-Einstein condensate suggests its full coherence at later times, it may also be argued that heat-

ing from trap vibrations and imperfections, collisions with background gas particles, or effects related to the quasi-one-dimensional nature of the waveguided atoms [18] can indeed cause the coherence to be spoiled after sufficient propagation times. Thus, our experimental goal was to measure quantitatively the coherence of this propagating atom beam at an arbitrary time after its launch.

We made use of direct absorption imaging of the propagating atom beam to discern several properties of its evolution. Such imaging, applied along the symmetry axis of the circular waveguide, quantified the longitudinal linear density of the beam  $n(x)$  (Fig. 2c). From the growth of the spatial width  $\sigma_x$  of the beam vs. propagation time, we determined the rms momentum width as  $\sigma_p = m \times 1.8$  mm/s, a value within 10% of that expected due to the release of interaction energy in the launched Bose-Einstein condensate. This rms momentum width is obtained after  $\approx 10$  ms of mean-field acceleration, and would be expected to generate an atom beam highly correlated in momentum and position ( $\eta \simeq 1$ ). The transverse state of the atomic beam was characterized by suddenly releasing the atom beam from the waveguide and imaging the transverse extent of the beam after variable times of flight. These observations agreed well with a mean-field model of the coherent expansion of a Bose-Einstein condensate into a tight waveguide [19], and indicated the transverse state of the beam to be the ground state of the harmonic transverse confining potential after about 100 ms of propagation. The beam can thus be treated as one dimensional with its azimuthal state remaining unknown. Combining these observations, we obtain an upper bound on the longitudinal phase-space area of  $\mathcal{A}_{max} = 310\hbar$  for the beam after a half-revolution in the guide given its  $\sigma_x = 120 \mu\text{m}$  rms width at that stage.

This constraint on the phase-space area was greatly improved by application of SPPS to the propagating atom beam. For this, the probe and pump pulses were *both* obtained from a single beam propagating in the plane of the waveguide (to within  $\pm 1^\circ$ ), with a 0.4 mm beam diameter, a detuning 560 MHz below the  $^2S_{1/2}$ ,  $F = 1 \rightarrow ^2P_{3/2}$ ,  $F = 0$  transition, and circular polarization. A typical intensity of 10 mW/cm<sup>2</sup> was used, corresponding to observed single-particle Rayleigh scattering rates of 400 s<sup>-1</sup>, and pulses were typically 50  $\mu\text{s}$  in duration. After application of the superradiant pulses, the atoms were allowed to propagate further in the waveguide until the scattered atoms had clearly separated from the unscattered atoms (Fig. 2c-e). The fraction of scattered atoms and, hence, the total superradiant scattering rate from the pump-probe sequence, was then determined from the center of mass of the beam  $x_{CM}$  in the azimuthal coordinate. This approach has the benefit of being unaffected by atom-atom collisions in the guided cloud.

Such pump-probe spectroscopy was applied to the atom beam at different propagation times, and thus at different locations in the circular guide. As shown in Fig. 3, the measured coherence times depend strongly the position of the beam in the guide. Letting  $\phi$  measure the central an-

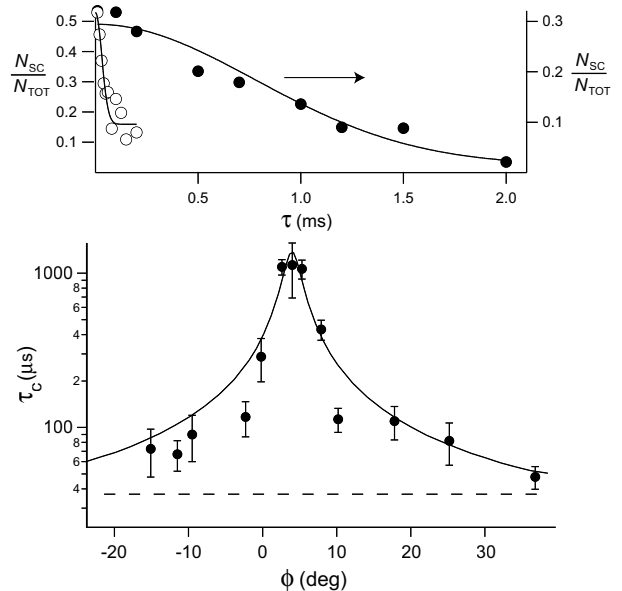


FIG. 3: Bichromatic SPPS of a quantum degenerate beam at approximately a half revolution in the circular waveguide. (a) SPPS at  $\phi = 38^\circ$  (open circles) and  $\phi = 4^\circ$  (closed circles) gives coherence times  $\tau_c = 47(8) \mu\text{s}$  and 1.1(1) ms, respectively, defined by the  $1/e$  decay time of the superradiant signal (Gaussian fits to data are shown). (b) Measured coherence times are compared to theoretical predictions for a coherent Gaussian beam (solid line) and an incoherent, uncorrelated ensemble (dotted line). The theoretical curve in fact predicts the maximum coherence time at  $\phi = 31^\circ$  (see text), but has been shifted for comparison to data.

gular position of the beam away from the point at which the pump/probe light is tangential to the guide, the superradiant response of atoms at large angles ( $|\phi| \gtrsim 20^\circ$ ) decays after a pump-probe delay time of around  $\tau = 50 \mu\text{s}$ , consistent with the coherence time discussed above for monochromatic SPPS determined by the overall momentum width of the beam. In contrast, for beam positions closer to  $\phi = 4^\circ$ , the coherence time is dramatically increased to over 1 ms, indicating coherence in the beam beyond that implied solely by the overall momentum width. Similar coherence times were observed after one, two, and three full revolutions around the ring.

This strong geometric dependence can be understood in the context of bichromatic SPPS. During the time  $\tau$  between application of the pump and probe pulses, the propagating atom beam rotates by an angle  $\Omega\tau$ , thereby varying the relative orientation between the incident light and the end-fire superradiant emission from the gas. Thus, expressed in a frame co-rotating with the atom beam, the superradiant recoil momenta of the pump and probe beams differ by  $\Delta\mathbf{q} \simeq k\Omega\tau (-\sin\phi\hat{x} + \cos\phi\hat{r})$ , with  $\hat{x}$  and  $\hat{r}$  being unit vectors in the azimuthal and radial transverse directions, respectively, and assuming  $\Omega\tau \ll 1$ .

With these approximations we apply the one-

dimensional treatment of bichromatic SPPS to this situation by considering just the contribution of longitudinal phase matching to superradiant scattering. SPPS applied to the rotating beam while at an angle  $\phi$  probes the Wigner function of the beam at a *constant* phase-space projection angle given by  $\tan \theta = \frac{m\Omega\sigma_x}{\sigma_p} \frac{\sin \phi}{1+\cos \phi}$ .

Using experimentally-measured quantities for the beam after a half revolution in the waveguide, the condition  $\tan \theta = 1$  for probing the homogeneous momentum width of the correlated atom beam is predicted to occur at  $\phi_c = 31^\circ$ . This value clearly does not match the experimentally observed  $\phi_c = 4(2)^\circ$  (Fig. 3b). 2D models which numerically evaluated the superradiance phase matching integral [11] showed that the beam curvature alone did not resolve this disagreement. Rather, to account for this discrepancy, we suspect it is necessary to adapt our 1D treatment of superradiance to beams with small Fresnel number, i.e. with length greatly exceeding the Rayleigh range defined by the probe wavelength and the transverse width of the atom beam. We suspect that our method may be probing only short portions of the beam, the momentum width of which is enhanced by their small extent, rather than probing the beam as a whole.

Despite the imperfect match between the 1D theory and the experimental data, the most important prediction of bichromatic SPPS in a rotating system — long coherence times at  $\phi < 0$  — is clearly evident in this system. We thus assert that the observations retain their relevancy as a probe of the phase-space distribution of the atom beam. From the maximum coherence time of  $\tau_c = 1.1(1)$  ms, we

obtain an empirical value of  $\eta = 1 - (4.9(6) \times 10^{-4})$  for the aforementioned correlation parameter. The atom beam is thus constrained to inhabit a phase-space area of no more than  $\mathcal{A} = 9(1)\hbar$ , equivalent to placing a lower bound of  $\mathcal{L} = (\hbar|\mathbf{q}|/m)\tau_c = 13(1)\mu\text{m}$  [14] on the longitudinal coherence length of the propagating cloud.

The maximum coherence time observed is plausibly limited not by the lack of longitudinal coherence, but rather by the decay of the superradiant scattering rate  $\Gamma(\tau)$  due to transverse phase matching. Assessing a 2D phase-matching integral with the transverse state being the non-interacting ground state of the transverse trapping potential, one finds an upper bound on the coherence time of  $\approx (2\Omega k\sigma_T \cos \phi)^{-1} < 1200\mu\text{s}$  with  $\sigma_T = \sqrt{\hbar/2m\omega_T}$  and  $\omega_T$  being the transverse trap frequency. Thus, our observations should be construed as placing quantitative lower bounds on the coherence of the propagating atom beam while remaining consistent with its complete coherence.

In conclusion, we have described bichromatic SPPS as a technique to perform tomography of the Wigner function of a propagating atom beam. We implemented this technique to probe an ultracold atomic beam propagating in a circular waveguide and observed long coherence times consistent with a highly degenerate quantum ensemble of  $3 \times 10^5$  atoms occupying no more than 10  $(\sigma_x/\mathcal{L})$  phase-space cells.

This work was supported by DARPA (Contract F30602-01-2-0524), ARO, and the David and Lucile Packard Foundation. KLM acknowledges support from NSF and SG from the Miller Institute.

- 
- [1] S. Gupta, K. Dieckmann, Z. Hadzibabic, and D. E. Pritchard, Phys. Rev. Lett. **89**, 140401 (2002).
  - [2] Y. Torii, Y. Suzuki, M. Kozuma, T. Sugiura, T. Kuga, L. Deng, and E. W. Hagley, Phys. Rev. A **61**, 041602(R) (2000).
  - [3] L. Deng, E. W. Hagley, J. Wen, M. Trippenbach, Y. Band, P. S. Julienne, J. E. Simsarian, K. Helmerson, S. L. Rolston, and W. D. Phillips, Nature **398**, 218 (1999).
  - [4] B. Eiermann, P. Treutlein, T. Anker, M. Albiez, M. Taglieber, K.-P. Marzlin, and M. K. Oberthaler, Phys. Rev. Lett. **91**, 060402 (2003).
  - [5] B. Eiermann, T. Anker, M. Albiez, M. Taglieber, P. Treutlein, K.-P. Marzlin, and M. K. Oberthaler, Phys. Rev. Lett. **92**, 230401 (2004).
  - [6] A. E. Leanhardt, A. P. Chikkatur, D. Kielpinski, Y. Shin, T. L. Gustavson, W. Ketterle, and D. E. Pritchard, Phys. Rev. Lett. **89**, 040401 (2002).
  - [7] E. Wigner, Phys. Rev. **40**, 749 (1932).
  - [8] D. Leibfried, D. M. Meekhof, B. E. King, C. Monroe, W. M. Itano, and D. J. Wineland, Phys. Rev. Lett. **77**, 4281 (1996).
  - [9] C. Kurtsiefer, T. Pfau, and J. Mlynek, Nature **386**, 77 (1997).
  - [10] S. Gupta, K. W. Murch, K. L. Moore, T. P. Purdy, and D. M. Stamper-Kurn, Phys. Rev. Lett. **95**, 143201 (2005).
  - [11] S. Inouye, A. P. Chikkatur, D. M. Stamper-Kurn, J. Stenger, and W. Ketterle, Science **285**, 571 (1999).
  - [12] Y. Yoshikawa, Y. Torii, and T. Kuga, Phys. Rev. Lett. **94**, 083602 (2005).
  - [13] N. E. Rehler and J. E. Eberly, Physical Review A **3**, 1735 (1971).
  - [14] B. Saubamea, T. W. Hijmans, S. Kulin, E. Rasel, E. Peik, M. Leduc, and C. Cohen-Tannoudji, Phys. Rev. Lett. **79**, 3146 (1997).
  - [15] S. Inouye, R. F. Löw, S. Gupta, T. Pfau, A. Görlitz, T. L. Gustavson, D. E. Pritchard, and W. Ketterle, Phys. Rev. Lett. **85**, 4225 (2000).
  - [16] J.-Y. Courtois, S. Guibal, D. R. Meacher, P. Verkerk, and G. Grynberg, Phys Rev Lett **77**, 40 (1996).
  - [17] K. W. Murch, K. L. Moore, S. Gupta, and D. M. Stamper-Kurn, Phys. Rev. Lett. **96**, 013202 (2005).
  - [18] K. Bongs, S. Burger, S. Dettmer, D. Hellweg, J. Arlt, W. Ertmer, and K. Sengstock, Phys. Rev. A **63**, 031602(R) (2001).
  - [19] L. Salasnich, A. Parola, and L. Reatto, Phys. Rev. A **65**, 043614 (2002).